ESTABLISHING A LIVE CARTILAGE-ON-CARTILAGE INTERFACE FOR TRIBOLOGICAL TESTING

Robert L. Trevino[a], **Jonathan Stoia**[b], **Michel P. Laurent**[b], **Carol A. Pacione**[b], **Susan Chubinskaya**[b,c], and **Markus A. Wimmer**[a,b]

[a]Department of Anatomy and Cell Biology, Rush University Medical Center, Chicago, IL

[b]Department of Orthopedic Surgery, Rush University Medical Center, Chicago, IL

[c]Department of Pediatrics, Rush University Medical Center, Chicago, IL

Abstract

Mechano-biochemical wear encompasses the tribological interplay between biological and mechanical mechanisms responsible for cartilage wear and degradation. The aim of this study was to develop and start validating a novel tribological testing system, which better resembles the natural joint environment through incorporating a live cartilage-on-cartilage articulating interface, joint specific kinematics, and the application of controlled mechanical stimuli for the measurement of biological responses in order to study the mechano-biochemical wear of cartilage. The study entailed two parts. In Part 1, the novel testing rig was used to compare two bearing systems: (a) cartilage articulating against cartilage (CoC) and (b) metal articulating against cartilage (MoC). The clinically relevant MoC, which is also a common tribological interface for evaluating cartilage wear, should produce more wear to agree with clinical observations. In Part II, the novel testing system was used to determine how wear is affected by tissue viability in live and dead CoC articulations. For both parts, bovine cartilage explants were harvested and tribologically tested for three consecutive days. Wear was defined as release of glycosaminoglycans into the media and as evaluation of the tissue structure. For Part I, we found that the live CoC articulation did not cause damage to the cartilage, to the extent of being comparable to the free swelling controls, whereas the MoC articulation caused decreased cell viability, extracellular matrix disruption, and increased wear when compared to CoC, and consistent with clinical data. These results provided confidence that this novel testing system will be adequate to screen new biomaterials for articulation against cartilage, such as in hemiarthroplasty. For Part II, the live and dead cartilage articulation yielded similar wear as determined by the release of proteoglycans and aggrecan fragments, suggesting that keeping the cartilage alive may not be essential for short term wear tests. However, the biosynthesis of glycosaminoglycans was significantly higher due to live CoC articulation than due to the corresponding live free swelling controls, indicating that articulation stimulated cell activity. Moving forward, the cell response to mechanical stimuli and the underlying mechano-biochemical wear mechanisms need to be further studied for a complete picture of tissue degradation.

Corresponding author: Rush University Medical Center, 1611 W. Harrison St., Ste. 204, Chicago, IL 60612, U.S.A., 1-312-942-2789 (phone), 1-312-942-4491 (fax), robert_trevino@rush.edu.

Conflicts of Interest: None

Keywords

cartilage; cartilage mechanics; tribology- wear; joint motion simulation

1. INTRODUCTION

Osteoarthritis is a debilitating disease of the entire joint, which takes several decades to progress and has multiple underlying etiologies. Cartilage degradation and wear is one possible component leading to joint failure, partly due to the limited capacity of cartilage to repair and regenerate itself[1]. For cartilage biotribology, friction and lubrication are more often assessed. The challenge of cartilage wear, as suggested in Katta, et al.[2], is due to the complexity of the underlying processes as wear and biochemical degradation are acting simultaneously.

Wear is classically defined as being the result of one of four major mechanisms: abrasion, adhesion, surface fatigue, and tribochemical reactions[3]. Of these, abrasion, adhesion, and surface fatigue are most often prescribed as the underlying mechanisms of cartilage wear[2]. Tribo-chemical wear, though, could play a major role in influencing cartilage degradation. However, the phrase lacks emphasis on how the biological factors, which include chondrocytes, enzymes, mechanotransduction, and inflammation, influence cartilage wear. *Mechano-biochemical wear* fully describes the complex interactions between mechanical forces and biological/chemical reactions. Such a concept acknowledges how load and mechanical forces are transduced to biochemical reactions and cellular responses via mechanotransduction and cell surface receptors. Because of this connection, we propose that *mechano-biochemical wear* is another important underlying wear mechanism for cartilage degradation that has yet to be fully explored.

A review of the current literature indicates that most existing in vitro models do not replicate three key tribological and biological aspects of the normal joint environment, which would impact the understanding of mechano-biochemical cartilage wear: (1) the articulating motion of surfaces, (2) an interface based on the cartilage-cartilage interaction, and (3) the biological responses to wear of living tissue. First, current in vitro models do not effectively mimic the tribological complexity of joint motion while also maintaining physiologic conditions[4]. The biomechanics of natural joints includes rolling and gliding motion at the cartilage surface with compressive, shear, and tensile stresses[5]. Models of cartilage mechanics apply loading conditions such as static or dynamic compression[6–9], shear forces[10–13], hydrostatic pressure[14], or supraphysiological impaction forces[15,16]. These models provide an incomplete picture of the tribological stresses at play in a joint by not simulating shear forces at the surface. Even basic tribological models utilizing pin-on-disc or flat-on-flat tribometers lack the rolling and gliding motion seen in vivo[2]. Limited studies have applied more complex mechanical patterns and loads to native cartilage tissue resulting in surface shear stress[17–21]. Second, in tribological testing, the biological cartilage-cartilage interface of a joint is often replaced by an interface of cartilage against glass or other biomaterials[22–26], neglecting the native tissue response to motion and loading against a naturally soft counterface. The few studies that do utilize a cartilage-on-

cartilage interface do so for studies of friction and/or lubrication[27,28], for comparison against chondroplasty materials[29,30], or for supraphysiological impaction[16]. Third, a final biological concern with many studies is the limited understanding of living cartilage response to tribological stresses as frozen or dead tissue has been typically used[21,31]. Eliminating the biological response from the system provides an incomplete picture of cartilage degradation. Studies may have replicated one or two of the three aspects listed above, such as through the use of dead cartilage-on-cartilage in a pin-on-pin configuration[31] or living tissue with complex compression and shear loading to evaluate gene response[12,32]. However, according to our literature review, no current study has replicated all three aspects together.

To improve the modeling of articulation of the native joint, the purpose of this study was to establish and begin validating a novel in vitro system utilizing a living cartilage-on-cartilage interface for wear testing that addresses the aforementioned features of the human joints missed in the existing models. There were two objectives for the study: (I) to design and test a system applying complex articulating motion to a living cartilage-on-cartilage (CoC) interface with comparison to a metal-on-cartilage (MoC) interface to evaluate system sensitivity; (II) to evaluate the effect of rolling and gliding motion on the biological response and its impact on matrix wear through comparing living and dead tissue. The MoC interface was chosen to evaluate system sensitivity because it is used clinically in hemiarthroplasties that are expected to last a decade, implying they produce only limited cartilage damage (but still more than CoC)[33–35]. In spite of this limited damage, a successful test set-up must be able to discriminate cartilage wear differences between the CoC and MoC pairings. For the second objective, we investigated wear differences between live and dead cartilage tissue. It has been reported that over time, frozen osteochondral grafts show deterioration of the graft properties in vivo, including cartilage softening, loss of matrix proteins, and an increase in surface irregularity, as compared to fresh grafts[36]. Because of this clinical observation, we hypothesized that the live CoC model would increase its biosynthetic activity compared to the non-wearing control tissue and show less matrix damage compared with dead tissue.

2. MATERIALS & METHODS

2.1 Cartilage Specimens

Cartilage from the stifle (knee) joint was obtained from steers (approximately 6–8 months old) that were slaughtered by a local abattoir 48 hours prior to requisition. Joints were kept intact and refrigerated before arrival to the lab. Joints were then dissected to expose the femoral trochlear groove, and visual integrity of the cartilage (i.e. lack of bruising) and synovial fluid (i.e. absence of blood) was confirmed prior to use. Baseline cell viability of a cartilage sample from the joint was also later evaluated before samples were used in tribological testing. At least 10 joints were used for each investigation.

Full thickness cartilage discs were removed with a custom oval punch (20 mm length x 14 mm width) from within the trochlear groove and trimmed through the deep zone to an approximate thickness of 3 mm (Fig. 1a). Discs were secured in semiconfined compression in porous polyethylene wafers, which were placed in polyether ether ketone (PEEK) specimen cups (Fig. 1b). To provide a cartilage counterface for the cartilage-on-cartilage

testing, cartilage strips (45 mm length x 8 mm width x 3 mm height) were removed with a scalpel from the trochlear rim, and then trimmed to exact size (Fig. 1c). Strips were secured to a custom Delrin® ball (Fig. 1d). The 28 mm ball has a 1 mm groove for the strip, which secures the strip against lateral displacement. In addition, the ends of the strip are fixed with either screws or silk surgical suture. Cartilage discs and strips were cultured in fresh DMEM: Ham's F-12 (1:1) media containing 1% Mini-ITS (50 mM insulin, 2 μg/mL transferrin, 2 ng/mL selenous acid, 25 μg ascorbic acid, and bovine serum albumin/linoleic acid at 420/2.1 μg/mL) and antibiotic solution (penicillin, streptomycin, amphotericin B, and gentamicin) at 37°C, 5% CO_2, 95% humidity.

2.2 Study Design

2.2.1 Tribological Apparatus Design—To address Objective (I) and (II), a cartilage-on-cartilage (CoC) articulating model needed to be created. The principle design of the tribological test simulator is detailed in Wimmer et al.[37] (Fig. 1e). Tribologically, the surface interaction in an articular joint is considered reciprocating sliding wear with a smaller contact area than the wear path. To represent this, a biaxial pin-on-ball concept was modified where a cell-seeded scaffold or cartilage tissue (the pin) in pressed onto a conforming ball. The motion trajectories of the two bodies were in phase difference, which when combined with cyclic compressive loading, produces complex shear force patterns on the surface of the scaffold/cartilage pin.

As the simulator was designed for studies with chondrocyte-seeded scaffolds, modifications were necessary to allow for cartilage testing. First, alterations were made to the cup placement to allow larger cartilage discs to provide a wear path and surrounding tissue. Additionally, for CoC articulation, the Delrin ball adapter for the cartilage strip was created to maintain the initial pin-on-ball concept and to create a similar contact point and wear path for CoC articulation and for metal-on-cartilage (MoC) articulation. This modification creates a wear path with a resulting wear scar that is roughly 40% of the total surface of the cartilage explant. Second, in order to introduce rolling and gliding motion, a migrating contact point with a speed of 0.5 mm/sec was introduced by creating a 10 mm offset between the normal load axis and the rotational axis of the disc (Figs. 1f–h). A migrating contact point has been shown to a) improve lubrication and to allow rehydration of the tissue[38] and b) improve cell viability at the point of contact over time in chondrocyte-seeded scaffolds[39] and in cartilage explants[40].

2.2.2 Objective I: System Validation of Cartilage-on-Cartilage as Compared to Metal-on-Cartilage—Cartilage was randomized to the following groups: unloaded, free-swelling control (FSC), tribological test against metal (MoC), or tribological test against cartilage (CoC). For the MoC tests, the metal counterface is a cobalt chromium head (32 mm diameter), which was selected due to its clinical role in hemiarthroplasty and its research role in in vitro wear testing[34,40,41]. After removal of tissue from the joint, all samples underwent a five-day preculture in culture media with daily changes and replenishing

2.2.3 Objective II: Comparison of Live and Dead Tissue in a Cartilage-on-Cartilage Model—Samples were randomized into four groups: live unloaded free-swelling

control (live FSC), live tribological test against cartilage (live CoC), dead unloaded free-swelling control (dead FSC), and dead tribological test against cartilage (dead CoC). Similar to Objective I, live tissue samples underwent a five-day preculture. For the dead tissue samples, both the cartilage disc and the cartilage strip underwent the following pre-treatment: on the first day after harvesting, samples experienced three freeze-thaw cycles, where a cycle consists of two hours storage in a −80°C freezer then forty-five minutes in the 37°C incubator, as adapted from Clements, et al.[42]. They found that three cycles at those temperature fluctuations would cause 100% cell death, which was confirmed in our laboratory with analysis of cell viability and metabolic response (for protocols see below). After freeze-thaw, samples were secured in the polyethylene platen/PEEK cup and cultured for the remainder of the preculture period like the live samples. The preculture period was followed by three days of tribological testing in the above assigned groups.

2.2.4 Tribological Protocol—After tissue procurement and the respective pre-treatment periods, cartilage samples underwent tribological testing in the simulator (Fig. 1e). The strip/ball apparatus and material heads were mounted onto the joint motion simulator with their respective discs. The four-station simulator is housed in a separate incubator which maintains testing conditions similar to the culture incubator at 37°C, 5% CO_2, and 95% humidity. Balls were manually lowered, and the discs were raised by a stepping motor to reach an approximate contact load of 45 N. The balls were rotated at a frequency of 0.5 Hz and stroke of 30°, while each explant was rotated at a frequency of 0.1 Hz and stroke of 15°. This dual rotation resulted in a rolling and gliding motion with a 20 mm^2 contact area creating a curvilinear path equivalent to 5.2 mm, which was identical for both the metal heads and the cartilage strip/ball adapter. The surface stresses were different due to the increased compliance of the cartilage strip counterface, but the loading regimes were the same. This mimics the situation in vivo where natural joint loads are similar to those acting on the bearing surfaces of arthroplasties. The test duration was three hours per day for three days. The culture medium from each sample was collected and replenished in full at the conclusion of each three-hour test; 3 mL of media for the discs and 12 mL for the strips were needed to fully submerge samples for the test and rest periods. Between test periods, cartilage was incubated overnight for a rest period with the medium collected and changed immediately before the next testing period. Upon collection, all media was stored at −80°C and analyzed individually. After completion of testing on day three, the wet weight of samples was recorded.

2.3 Analysis

2.3.1 Tissue Viability—Cartilage cell viability was examined to assess how it is affected by mechanical articulation[43]. In brief, immediately after day three of articulation, cartilage strips and discs were dissected parallel through their respective contact paths, stained with calcein AM and ethidium homodimer-1, and imaged with a confocal laser-scanning microscope (Nikon E200, Melville, NY) at 5x. Live and dead cell counts were obtained using Image J software[44]. The percentage of live cells was calculated by comparing the number of live cells to the total number of cells counted. The top 15% of the cartilage thickness was defined as the superficial zone[45].

2.3.2 Tissue Histology—After dissection through the wear path, cartilage samples were fixed in neutral buffered formalin, embedded in paraffin, sectioned at 5 μm, and stained with Safranin-O/fast green to evaluate tissue integrity, chondrocyte appearance, and matrix proteoglycan distribution[43]. Slides were imaged using a light microscope (Eclipse TE2000-S; Nikon Instruments Inc, NY) at 4x magnification. Additional samples were stained with Picrosirius red to evaluate the integrity of the collagen fibrils to identify any potential disruptions at the surface[46]. A light microscope with a polarization filter (Olympus BX40) was used to capture the birefringent optical properties of the samples, which indicate orientation of the fibers.

2.3.3 Tissue Surface Topography—Immediately after testing, the integrity and wear of the articular surface was evaluated using a scanning white light interferometry microscope (NewView 6300; Zygo Corp., Middlefield, CT) for non-contact surface topography measurements with a previously published protocol[43]. The topography data was corrected for sample geometry (curvature) to yield an array of deviations around the center/wear area surface, from which the surface roughness parameters Ra, SRz, PV, and Rsk were computed (MetroPro version 8.1.5, Zygo Corp.). Ra is the mean arithmetic deviation from the center surface. SRz is the average peak-to-valley areal roughness, which is the average of Rz values computed over the areal data array. Each Rz value is the arithmetic average of the five highest peaks and the five lowest valleys along a radial line going through the center of the areal data array. PV or maximum the peak-to-valley depth, equals the most positive minus the most negative deviation on the surface. Rsk, the areal skewness, is a measure of the symmetry of the deviations about the center surface, negative skew being associated with a prevalence of valleys and positive skew with a prevalence of peaks.

2.3.4 Tissue Metabolism—Metabolic activity of chondrocytes after three days of testing was investigated using the incorporation of radiolabeled $^{35}SO_4$ as described in Masuda et al. [47]. Immediately after day three testing, 4 mm diameter, full thickness plugs from the center/wear area were labeled by incubating with fresh media containing the radiolabeled sulfate for a period of four hours and then rinsed with clean media. Following the labeling, the media was collected and tissue samples digested overnight with a 20 μg/mL papain solution. Radioactivity of the labeling media and digested samples was then quantified via a scintillation counter. Values were normalized to wet weight of the tissue prior to labeling and are presented as normalized to the respective live unloaded FSC to control for animal differences.

2.3.5 Sulfated-Glycosaminoglycan (GAG) Content—To evaluate the effect of articulation on proteoglycan content in collected media and tissue, the dimethylmethylene blue (DMMB) dye reaction was used[48,49]. For both Objective I and Objective II, media samples from individual collection time points were analyzed separately. Dye absorbance was measured at 530 nm and 595 nm using a spectrophotomorphic plate reader with bovine nasal septum as the standard (BCO-3015; Axxora Platform, San Diego, CA). GAG content of collected media was normalized to the number of interacting cartilage surfaces. After papain digestion, GAG content of tissue plugs was normalized to the wet weight of the sample.

2.3.6 Hydroxyproline (HYP) Content—HYP has commonly been used as a marker of collagen matrix disruption[50]. Pooled aliquots of media from control and test samples in Objective I were lyophilized for determination of HYP content via reversed-phase high performance liquid chromatography (RP-HPLC). 10 μL of the processed mixture was used for analysis with a fluorometric detector set at an excitation wavelength of 263 nm and an emission wavelength of 313 nm. Calibration was performed by linear regression using external standard solutions based on peak height. HYP content of the media was normalized to the number of cartilage surfaces.

2.3.7 Aggrecan Fragment Released into Media—The Western blot technique was used to detect the presence of different aggrecan fragments released into the media through utilizing gel electrophoresis to separate proteins of different molecular weights. Through the chondrocyte response to mechanotransduction, enzymes cause cleavage of the aggrecan core protein (see Fig. 2 for potential cleavage sites), creating smaller protein fragments which can be released into the medium and then detected with biochemical techniques. Aliquots of media (20 μL) were deglycosylated with a buffered solution including keratanase I, keratanase II, and chondroitinase ABC (Seikagaku Inc., Japan). Ladder standard (10 μL) and samples (15 μL) were loaded in a Bis-Tris SDS-PAGE pre cast gel (4–12% 1.0 mm thick, 15 well) with a company SDS running buffer and antioxidant (Invitrogen). Electrophoresis run time was 50 minutes at 200 V with approximately 110–125 mA at the start and 70–80 mA at the end. A PVDF membrane was pre-soaked in methanol for activation and was placed with the gel in a transfer cell with ice-cold transfer buffer with 15% methanol for 1.5 hours at 100 V. After transfer, the gel was stained with Simply Blue (Thermo Fisher Scientific, Waltham, MA) for confirmation of loading. The PVDF membrane was blocked in BSA. Primary antibodies (mouse monoclonal AHP0022 (Invtirogen, Carlsbad, CA) at 1:500 concentration, rabbit polyclonal anti-AGEG neoepitope antibody to the N-terminus [1820]AGEG (from human sequence) as previously described[51] (kindly provided by Dr. Anne-Marie Malfait, Rush University) at 1:1000 concentration) were diluted in 25 mL of BSA with TBS-tween and incubated overnight at 4°C. After washing, secondary antibody (conjugated to alkaline phosphatase (AP) at 1 1:5000 concentration) was diluted in BSA and place on rollers for 1 hour at room temperature. After washing with TBS-tween, the ProtoBlot II AP System (Promega, Fitchburg, WI), a commercial colormetric substrate kit, was used for rapid protein detection on the membrane as the bands turn dark purple because of the AP activity.

Two antibodies were used in this study for detecting aggrecan fragments [Fig. 2]. The affinity for AHP0022 is the hyaluronic binding region of the globular domain (G1, G2, G3) of the aggrecan core protein. Because of enzymatic cleavage by ADAMTS at other sites on the core protein as denoted in Figure 2, multiple sized bands can be detected as long as they contain a globular domain. AHP0022 has been used in clinical research in evaluating aggrecan fragments present in patient synovial fluid[52,53]. Anti-AGEG binds to a small fragment at the G3-end of the aggrecan core protein that is also enzymatically cleaved[51]. Using a combination of these two antibodies provides a wide coverage of potential aggrecan fragments released into the media.

2.4 Statistics

Data are presented as mean +/− standard error of the mean (SEM) with n=12 samples per group in each aim. For the GAG and HYP released into media, data were normalized to the cartilage surfaces in contact, meaning CoC values were divided by two. In the design of the CoC model, the surface area of the cartilage discs and strips in contact with the media is similar, leading to the assumption that the cartilage disc and strip contribute equally to the GAG release. Normal distribution of data was confirmed with normality plots. For Objective I, a one-way ANOVA was used to compare the three groups (FSC, CoC, and MoC). For Objective II, a student t-test was used to analyze the $^{35}SO_4-$ incorporation while a two-way ANOVA compared the groups for GAG release and GAG content. P 0.05 was deemed significantly different. Analyses were conducted with GraphPad Prism6 (GraphPad Software, La Jolla, CA).

3. RESULTS

3.1 Objective I: System Validation of CoC as Compared to MoC

3.1.1 Assessment of Chondrocytes: Cell Viability—Tissue viability was maintained throughout the culture period, as evidenced by the FSC samples with viability >85% (Table 1). Articulation against cartilage did not cause additional cell death and the percentage of viable cells was comparable between FSC and CoC (Figs. 3a & 3c). However, articulation against cobalt chromium in the MoC group induced a layer of dead cells at the surface (Fig. 3b), causing a significant loss in cell viability in the superficial zone (p<0.0001) and throughout the full depth of the tissue sample, termed "total depth viability" that also includes the superficial zone chondrocytes (p<0.0001) as compared to the FSC group. Similarly, MoC viability was significantly decreased compared to CoC at both the surface and the total depth (p<0.0001).

3.1.2 Assessment of Extracellular Matrix: Histology and Surface Topography—MoC samples displayed an increase in the surface damage and decreased Safranin-O staining in the middle zone as compared to FSC and CoC (Fig. 3d–f). In addition to surface damage, the superficial zone contained empty lacunae due, perhaps, to displacement of superficial zone chondrocytes. However, only little disruption of the collagen matrix at the surface was detected in all three experimental groups, FSC, MoC, or CoC, as seen when stained with Picrosirius red (Figs. 3g–i).

Topographical maps of the wear areas indicate more fibrillations for the MoC samples than the CoC samples (Figs. 3k–l). Surface fibrillations were not evident on the FSC samples (Fig. 3j). Surface roughness parameters Ra, PV, and Rsk were similar between the groups (Table 2). SRz, however, was significantly greater for MoC than for FSC (FSC: 1.412 +/− 0.147μm; MoC: 2.761 +/− 0.284 μm; p=0.0013). There was no difference between CoC with FSC (CoC: 2.193 +/− 0.283 μm; p=0.092).

3.1.3 Assessment of Cartilage Wear: GAG and HYP Release into Media during Articulation—Measuring GAG and HYP release into the media for proteoglycans and collagen provide a biochemical proxy for evaluation of cartilage matrix wear. GAG release

into the media (Fig. 4a) was significantly higher for the MoC group (599.7 +/− 63.43 μg/mL) than for the FSC (342.0 +/− 52.74 μg/mL) and CoC groups (370.7 +/− 27.03 μg/mL) (MoC vs. FSC: p=0.0026; MoC vs. CoC: p=0.0077). There was no difference detected between the FSC and CoC groups. HYP release into the media (Fig. 4b) followed a similar pattern as GAG with MoC (28.18 +/− 1.93 μg/mL) being significantly greater than for FSC (19.03 +/− 1.65 μg/mL) and CoC (16.14 +/− 0.82 μg/mL) (MoC vs. FSC: p=0.001; MoC vs. CoC: p=0.0001).

3.2 Objective II: Comparison of Live and Dead Tissue in a CoC Model

3.2.1 Assessment of Chondrocytes: Cell Viability and Metabolism—No differences in chondrocyte viability were observed between the live FSC and the live CoC samples, as seen in objective I (Table 3). The dead FSC and dead CoC samples were confirmed with no live cells present.

Samples were analyzed for metabolic activity immediately following the final test period. Dead samples were confirmed if resulting CPM was below a background threshold. As normalized to the respective FSC, the load and articulation motion produced a significant increase in $^{35}SO_4$-incorporation in both the live CoC disc (1.50 +/− 0.139; p=0.009) and live CoC strip (1.44 +/− 0.139; p=0.015) in comparison to live FSC (Fig. 5).

3.2.2 Assessment of Extracellular Matrix: Histology and GAG Content Retained—There was no difference in histological staining for GAG content when comparing live versus dead articulated samples using Safranin-O. Similarly, no differences in collagen architecture were detected with Picrosirius red. The GAG content of cartilage plugs removed from the wear area was not significantly different between groups (p=0.553 for viability factor, p=0.593 for articulation factor (Fig. 6a)).

3.2.3 Assessment of Cartilage Wear: GAG and Aggrecan Fragment Release into Media—No differences were detected in GAG release due to chondrocyte viability when comparing samples after tribological testing (live CoC: 349.0 +/− 68.41 μg/mL; dead CoC: 333.4 +/− 42.65 μg/mL; p=0.998). This was also true when evaluating GAG release with the unloaded, free-swelling controls (live FSC: 400.8 +/− 80.97 μg/mL; dead FSC: 292.5 +/− 29.87 μg/mL; p=0.570). Additionally, there were no differences due to articulating motion when comparing CoC to the respective FSC (live FSC versus live CoC: p=0.925; dead FSC versus dead CoC: p=0.961 (Fig. 6b)).

Two antibodies were used to analyze aggrecan fragments released into the media. One, AHP0022, shows affinity for the hyaluronic acid binding region within the interglobular domains in the proteins of aggrecan (G1, G2, G3). As such, this antibody produces multiple bands on Western blotting, representing aggrecan fragments of different molecular weights[52,53] and demonstrated schematically in Figure 2. Here, subtle differences can be detected between the testing groups. In Figure 7a, all testing groups produced bands A–D with varying intensities. Both live and dead test groups appeared to have darker bands than their respective controls, suggesting higher concentrations of similarly weighted proteins. Additionally, bands A & B appeared visually darker in live samples than the respective dead samples while band C appeared darker in the dead samples. There also appeared to be

differences in the molecular weights of the predominant bands released in the controls. For live control, bands A and B appear more intense while for dead control, bands B and C appear more intense. The similar comparisons are seen for the anti-AGEG, which produces a single specific aggrecan fragment (Fig. 7b).

4. DISCUSSION

The purpose for this study was to create a novel in vitro system for testing cartilage mechano-biochemical wear that applies articulation and load to a living cartilage-on-cartilage interface. We outlined three potential limitations present in the existing in vitro models of joint motion: insufficient modeling of complex articulating motion, the limited use of cartilage-cartilage articulating interfaces, and minimization of the biological influence on wear by using dead cartilage. We successfully created a joint motion simulator that addresses the aforementioned limitations through its use of dual-axial rotation with rolling and gliding motion on live cartilage explants. Initially, we compared the live CoC to a live MoC model and found that the CoC model caused no detrimental effects on the chondrocytes, extracellular matrix, and matrix wear, performing more similarly to the FSC samples and having more favorable outcomes in terms of tissue preservation than the MoC samples. We subsequently compared live and dead CoC models in a wear test to determine the relationship between tissue viability on matrix wear and structure, finding surprisingly little difference between the two models. Yet, articulation increased biosynthetic activity of live chondrocytes during articulation in comparison to non-articulated, free-swelling controls, indicating a biochemical response that needs to be further investigated in future studies.

Our model is in line with other in vitro work and animal studies while continuing to improve the replication of the in vivo joint motion and articulation through modeling the complex motion of natural joints and through the use of a physiological cartilage-on-cartilage interface. First, the joint motion simulator is intended to highlight the multi-axial loading with dynamic compressive-shear strains as seen in vivo when the femoral and tibial surfaces interact at migrating contact points due to the sliding and rolling of both surfaces in different stances in gait[38]. In addition to this motion, the mechanical forces experienced at the joint level also include interstitial flow and matrix compression and shear[5]. The senior author and several groups have utilized multi-axial loading devices and complex motion apparatus to evaluate tissue engineered constructs[4,37,39,54,55], yet these systems have been less frequently applied in the context of cartilage tissue. Second, other cartilage-on-cartilage models exist within the study of friction and lubrication[25,29,56] or for supraphysiological impaction[16], but these models may use simple motion patterns or not evaluate the influence of the biological response on wear. Further, the applied load of 45N results in a contact stress in excess of 2 MPa to the cartilage discs, in rage with in vivo findings[40]. Physiological loads experienced by cartilage at the hip[57,58] or knee[59] have been measured to be about 1 MPa during standing with peaks of 5 – 10 MPa during walking. It is also important to note that MoC models have been shown to experience higher contact stresses and frictional forces[19,56], as well as higher impact stress[16], when compared to CoC models. The stress differences highlight the need to use CoC for understanding natural joint wear.

Our newly developed model also highlights the following key aspects of relevance to in vivo applications. First, while no statistical differences in surface roughness were detected, the cartilage-on-cartilage interface showed improved matrix wear properties as compared to cobalt chromium, a commonly used material in hemiarthroplasty work and in vitro settings as a counterface. Secondly, the use of living tissue brought to light that cell viability at the surface suffers in the case of cobalt chromium. Although the specific mechanisms are unclear, it might be related to ion release or increased shear stresses. Furthermore, while our model did not replicate the observed damage of frozen osteochondral grafts in vivo over a long period[36], the relative equality of live and dead tissue in the bioreactor is consistent with observations made in a short-term in vitro study by Torzilli et al.[60]. Perhaps dead tissue may work in the short term, but will fail in the long term. Live tissue is also necessary for the evaluation of the biological mechanisms impacted by mechanical articulation. In this study, only the $^{35}SO_4$-incorporation was used as a biological indicator, but in future studies, gene analysis and proteomics should be utilized to evaluate the underlying mechanisms of cartilage mechanotransduction.

Multiple methods were utilized in Objective I to evaluate the cartilage wear. First, there was an increased release of both GAG and HYP for MoC articulation, which is in line with the other studies with simple motion[25] or animal models[34,41]. When compared to other in vitro wear systems utilizing physiological loads[61], the wear profiles of mechanically loaded CoC and FSC were similar. Both histological evaluation[62–64] and visualization of surface changes[43,65–67] have also been used in tribology to characterize wear. Histologically, MoC samples displayed an increase in the matrix disruption of aggrecan and GAG (Safranin-O staining) and little disruption in the collagen matrix (Picrosirius red staining). In contrast, no differences at the surface or throughout the extracellular matrix were observed between CoC and FSC. However, evaluation of surface changes with the more sensitive measurement from white light interferometry revealed that compared with FSC, CoC and MoC caused increased roughness as shown in the higher SRz, Rsk, and PV values; however, only the SRz increase for the MoC samples was statistically significant. Of the four surface roughness parameters that were considered, SRz (average of many local PV values) is expected to be the most sensitive to increasing surface fibrillation because it captures occasional but persistent deviations from smoothness that get lost with the Ra (arithmetic average of all deviations) and PV (depends on only two points over the whole data array). This finding suggests that the surface of cartilage is susceptible to microscopic changes in roughness due to articulation, regardless of counterface, but that these changes in roughness are not directly related with matrix disruption as seen with the CoC samples. Further studies are necessary to elucidate the relationship between surface damage and matrix degradation.

In Objective II, tissue viability played a significant role in evaluating the impact of mechanical articulation upon the biological metabolic response. Here, as expected, articulated living CoC samples had an increased $^{35}SO_4$-incorporation as compared to the non-articulated FSC samples. These findings support numerous studies that report the increase in metabolic activity due to mechanical stimulation[6,7,68,69]. Contrary though, in a study utilizing cartilage explants undergoing multiaxial compression with shear stresses, Heiner and Martin[18] found a decrease in $^{35}SO_4$-incorporation. The authors suggest that

their findings may be a result of limited interstitial fluid flow due to their device structure. They surmise that greater flow would likely stimulate matrix synthesis. Furthermore, their use of osteoarthritic human tissue could also explain the differences. Due to our use of healthy, young (bovine) tissue and the creation of a migrating contact point that keeps the fluid pressure[38], our study does not show such limitations.

In contrast to its effect on the metabolic response, tissue viability did not influence matrix wear as there was no significant difference in GAG release between the live and dead CoC articulating samples and the live and dead FSC samples. Furthermore, as there were no differences when comparing articulating samples to FSC, the GAG release was not influenced by articulating motion with a healthy cartilage counterface. This observation is consistent with the similar GAG content and histology of the live and dead tissue samples from the CoC wear tests. Perhaps, in order to elicit differences between live and dead tissues with respect to these outcome measures, the chondrocyte activity kinetics require much longer test times to translate into matrix damage. In humans, this process takes years, while in animal models, *e.g.* mouse, it can take several weeks[70]. Additionally, there may be different mechanisms regulating the GAG release in FSC and articulated CoC samples. Regardless, the results suggest that in short term wear tests, tissue viability does not influence GAG as a marker of wear. However, if cartilage wear is influenced by both mechanical stimuli and biological response via mechano-biochemical mechanisms, then chondrocyte viability is necessary for a complete understanding of wear. A logical next step would be further studies to evaluate the response at the cellular level, such as through gene expression and larger genomic or proteomic arrays.

The lack of influence of viability was comparable to the findings from Torzilli and Grigiene[60], the only other study evaluating live versus dead tissue via mechanical loading. There, they used a continuous cyclic loading model with mature bovine tissue under physiological conditions to separate the effects of catabolism and mechanical load. Although the authors made no statistical comparisons between test groups, no differences were seen for the effect of compressive loading on the live and dead samples. However, their cyclic loading actually significantly reduced GAG release and compared to respective precultured-only, non-tested samples, i.e. free swelling controls. This discrepancy between controls and test samples could be due to the differences in animal age or testing regime. Cyclic loading used by Torzilli and Grigiene[60] required the entire surface to be compressed with a porous platen while our system creates a central wear path on the surface with the remainder unloaded. This design difference could define the difference in surface area under compressive stress and potentially differences in rates of GAG release through the superficial zone.

Tissue viability also did not have an impact on wear as defined by the release of aggrecan fragments due to articulation. During natural degradation and wear of articular cartilage (i.e. osteoarthritis), cleavage of the aggrecan core protein is a common observation. Utilizing aggrecan fragments based on enzymatic degradation (such as by the ADAMTS family) as markers of wear would be a more clinically relevant biomarker than GAG release, as suggested by individual clinical studies[52,53,71] and larger biomarker reviews[72]. Both AHP0022[52,53] and anti-AGEG[71] have been evaluated as potential OA biomarkers in

patient studies. Fortunately, the immature bovine samples in this study produced similar sized bands as expected. Here, articulated samples (both live and dead test) produced a different banding pattern than the FSC samples. This could suggest that the mechanism of release related to mechanical loading and wear is different from non-wear release. It has been previously suggested that that GAGs released into the media due to mechanical testing vary in size[73]. Furthermore, changes to both the catabolic state via the release of enzymatically cleaved proteoglycans and the anabolic state via newly synthesized GAG contribute to the diversity of GAGs released into the media[74].

There are several limitations with the model and analysis presented here. First, though immature bovine tissue is commonly used for many reasons (e.g. thicker tissue, more readily available), the translatability of results to mature human cartilage has to be investigated as the biological and mechanical properties of immature and mature tissues are known to differ[75–77]. Secondly, our model only addresses the short-term effects of prescribed loads and motions on cartilage articulation. The biological and mechanical influence of other joint components, including the synovium and synovial fluid, the subchondral bone, and the meniscus, are not modeled as of yet. From an analytical perspective, follow-up on the mechanical properties of the cartilage samples is needed to fully characterize the tribological significance of our system. Also, a more semi-quantitative analysis of the enzymatically cleaved aggrecan fragments could further the discussion regarding the catabolic effects on matrix turnover. Lastly, while GAG and HYP are both commonly used markers of wear and are linked to the metabolism and histological analysis in this study, other potential wear markers with a greater clinical relevance should be considered. For instance, COMP has shown to be sensitive to mechanical loading, as demonstrated in clinical exercise studies[78,79], and collagen fragments have been used as structural markers of injury[80].

5. CONCLUSION

In conclusion, we established an in vitro cartilage-on-cartilage system for tribological testing that emulates physiological loading conditions. Our system models in vivo joint articulation using multi-axial rotation with a migrating contact point. By maintaining tissue viability, there is the potential to evaluate the mechano-biochemical wear processes through the biological response to mechanical loading and dissect the mechanotransduction pathways that link the mechanical signals to biological outputs. With the growing use of gene analysis and proteomics, future work will potentially distinguish the individual roles of the cellular and mechanical components. Although our data suggest that keeping the tissue alive does not directly influence short-term wear experiments as determined from GAG release and tissue histology, they also suggest that tribological stress stimulates biosynthetic activity, which could only be observed by using live tissue. As our metal-on-cartilage tissue demonstrated, our system can also be used to evaluate cartilage-friendly materials articulating against native cartilage, with the live cartilage-on-cartilage model serving as the benchmark as to further evaluate the impact of artificial materials upon matrix metabolism. Such evaluation would be useful for mechanistic and translational studies. Optimal in vitro models of cartilage articulation will account for the biological processes and the complex mechanical interactions to better understand the early processes of cartilage wear and

degradation. In the future, the underlying mechanisms will be further evaluated with analysis of gene expression changes and proteomic activity.

Acknowledgments

References

1. Zhang L, Hu J, Athanasiou KA. The Role of Tissue Engineering in Articular Cartilage Repair and Regeneration. Crit Rev Biomed Eng. 2009; 37:1–57. [PubMed: 20201770]

2. Katta J, Jin Z, Ingham E, Fisher J. Biotribology of articular cartilage—A review of the recent advances. Med Eng Phys. 2008; 30:1349–1363. DOI: 10.1016/j.medengphy.2008.09.004 [PubMed: 18993107]

3. Rabinowicz, E. Friction and Wear of Materials. 2. Wiley-Interscience; New York, NY: 1995.

4. Waldman SD, Couto DC, Grynpas MD, Pilliar RM, Kandel RA. Multi-axial mechanical stimulation of tissue engineered cartilage: review. Eur Cell Mater. 2007; 13:66–73. discussion 73–74. [PubMed: 17429796]

5. Mankin, H., Mow, VC., Buckwalter, JA., Iannotti, J., Ratcliffe, A. Orthop Basic Sci. Vol. Chapter 1. American Academy of Orthopaedic Surgeons; Columbus, OH: 1994. Form and function of articular cartilage; p. 1-44.

6. Sah RL, Kim YJ, Doong JY, Grodzinsky AJ, Plaas AH, Sandy JD. Biosynthetic response of cartilage explants to dynamic compression. J Orthop Res. 1989; 7:619–636. DOI: 10.1002/jor.1100070502 [PubMed: 2760736]

7. Kim YJ, Sah RL, Grodzinsky AJ, Plaas AH, Sandy JD. Mechanical regulation of cartilage biosynthetic behavior: physical stimuli. Arch Biochem Biophys. 1994; 311:1–12. DOI: 10.1006/abbi.1994.1201 [PubMed: 8185305]

8. Wong M, Siegrist M, Cao X. Cyclic compression of articular cartilage explants is associated with progressive consolidation and altered expression pattern of extracellular matrix proteins. Matrix Biol J Int Soc Matrix Biol. 1999; 18:391–399.

9. Aufderheide AC, Athanasiou KA. A direct compression stimulator for articular cartilage and meniscal explants. Ann Biomed Eng. 2006; 34:1463–1474. DOI: 10.1007/s10439-006-9157-x [PubMed: 16897420]

10. Lane Smith R, Trindade MC, Ikenoue T, Mohtai M, Das P, Carter DR, Goodman SB, Schurman DJ. Effects of shear stress on articular chondrocyte metabolism. Biorheology. 2000; 37:95–107. [PubMed: 10912182]

11. Jin M, Frank EH, Quinn TM, Hunziker EB, Grodzinsky AJ. Tissue shear deformation stimulates proteoglycan and protein biosynthesis in bovine cartilage explants. Arch Biochem Biophys. 2001; 395:41–48. DOI: 10.1006/abbi.2001.2543 [PubMed: 11673864]

12. Fitzgerald JB, Jin M, Grodzinsky AJ. Shear and compression differentially regulate clusters of functionally related temporal transcription patterns in cartilage tissue. J Biol Chem. 2006; 281:24095–24103. DOI: 10.1074/jbc.M510858200 [PubMed: 16782710]

13. Motavalli M, Akkus O, Mansour JM. Depth-dependent shear behavior of bovine articular cartilage: relationship to structure. J Anat. 2014; doi: 10.1111/joa.12230

14. Hall AC, Urban JPG, Gehl KA. The effects of hydrostatic pressure on matrix synthesis in articular cartilage. J Orthop Res. 1991; 9:1–10. DOI: 10.1002/jor.1100090102 [PubMed: 1984038]

15. Loening AM, James IE, Levenston ME, Badger AM, Frank EH, Kurz B, Nuttall ME, Hung H-H, Blake SM, Grodzinsky AJ, Lark MW. Injurious mechanical compression of bovine articular cartilage induces chondrocyte apoptosis. Arch Biochem Biophys. 2000; 381:205–212. DOI: 10.1006/abbi.2000.1988 [PubMed: 11032407]

16. Heiner AD, Smith AD, Goetz JE, Goreham-Voss CM, Judd KT, McKinley TO, Martin JA. Cartilage-on-cartilage versus metal-on-cartilage impact characteristics and responses. J Orthop Res. 2013; 31:887–893. DOI: 10.1002/jor.22311 [PubMed: 23335281]

17. Frank EH, Jin M, Loening AM, Levenston ME, Grodzinsky AJ. A versatile shear and compression apparatus for mechanical stimulation of tissue culture explants. J Biomech. 2000; 33:1523–1527. DOI: 10.1016/S0021-9290(00)00100-7 [PubMed: 10940414]

18. Heiner AD, Martin JA. Cartilage responses to a novel triaxial mechanostimulatory culture system. J Biomech. 2004; 37:689–695. DOI: 10.1016/j.jbiomech.2003.09.014 [PubMed: 15046998]

19. Northwood E, Fisher J. A multi-directional in vitro investigation into friction, damage and wear of innovative chondroplasty materials against articular cartilage. Clin Biomech Bristol Avon. 2007; 22:834–842. DOI: 10.1016/j.clinbiomech.2007.03.008

20. Schätti OR, Marková M, Torzilli PA, Gallo LM. Mechanical loading of cartilage explants with compression and sliding motion modulates gene expression of lubricin and catabolic enzymes. Cartilage. 2015; 6:185–193. DOI: 10.1177/1947603515581680 [PubMed: 26175864]

21. Schätti OR, Gallo LM, Torzilli PA. A model to study articular cartilage mechanical and biological responses to sliding loads. Ann Biomed Eng. 2015; doi: 10.1007/s10439-015-1543-9

22. Simon WH. Wear properties of articular cartilage in vitro. J Biomech. 1971; 4:379–389. [PubMed: 5171642]

23. Ewald FC, Sledge CB, Corson JM, Rose RM, Radin EL. Giant cell synovitis associated with failed polyethylene patellar replacements. Clin Orthop. 1976:213–219. [PubMed: 767030]

24. Kawalec JS, Hetherington VJ, Melillo TC, Corbin N. Evaluation of fibrocartilage regeneration and bone response at full-thickness cartilage defects in articulation with pyrolytic carbon or cobalt-chromium alloy hemiarthroplasties. J Biomed Mater Res. 1998; 41:534–540. [PubMed: 9697025]

25. Schwartz CJ, Bahadur S. Investigation of articular cartilage and counterface compliance in multi-directional sliding as in orthopedic implants. Wear. 2007; 262:1315–1320. DOI: 10.1016/j.wear.2007.01.007

26. Katta J, Jin Z, Ingham E, Fisher J. Effect of nominal stress on the long term friction, deformation and wear of native and glycosaminoglycan deficient articular cartilage. Osteoarthritis Cartilage. 2009; 17:662–668. DOI: 10.1016/j.joca.2008.10.008 [PubMed: 19028431]

27. Forster H, Fisher J. The influence of loading time and lubricant on the friction of articular cartilage. Proc Inst Mech Eng [H]. 1996; 210:109–119.

28. Schmidt TA, Gastelum NS, Nguyen QT, Schumacher BL, Sah RL. Boundary lubrication of articular cartilage: Role of synovial fluid constituents. Arthritis Rheum. 2007; 56:882–891. DOI: 10.1002/art.22446 [PubMed: 17328061]

29. Northwood E, Fisher J, Kowalski R. Investigation of the friction and surface degradation of innovative chondroplasty materials against articular cartilage. Proc Inst Mech Eng [H]. 2007; 221:263–279.

30. Li F, Su Y, Wang J, Wu G, Wang C. Influence of dynamic load on friction behavior of human articular cartilage, stainless steel and polyvinyl alcohol hydrogel as artificial cartilage. J Mater Sci Mater Med. 2010; 21:147–154. DOI: 10.1007/s10856-009-3863-5 [PubMed: 19756967]

31. Verberne G, Merkher Y, Halperin G, Maroudas A, Etsion I. Techniques for assessment of wear between human cartilage surfaces. Wear. 2009; 266:1216–1223. DOI: 10.1016/j.wear.2009.03.042

32. Fitzgerald JB, Jin M, Chai DH, Siparsky P, Fanning P, Grodzinsky AJ. Shear- and compression-induced chondrocyte transcription requires MAPK activation in cartilage explants. J Biol Chem. 2008; 283:6735–6743. DOI: 10.1074/jbc.M708670200 [PubMed: 18086670]

33. Jung M, Wieloch P, Lorenz H, Gotterbarm T, Veyel K, Daniels M, Martini AK, Daecke W. Comparison of cobalt chromium, ceramic and pyrocarbon hemiprosthesis in a rabbit model: Ceramic leads to more cartilage damage than cobalt chromium. J Biomed Mater Res B Appl Biomater. 2008; 85:427–434. DOI: 10.1002/jbm.b.30961 [PubMed: 17973249]

34. Custers RJH, Dhert WJA, Saris DBF, Verbout AJ, van Rijen MHP, Mastbergen SC, Lafeber FPJG, Creemers LB. Cartilage degeneration in the goat knee caused by treating localized cartilage defects with metal implants. Osteoarthritis Cartilage. 2010; 18:377–388. DOI: 10.1016/j.joca.2009.10.009 [PubMed: 19880000]

35. Oungoulian SR, Durney KM, Jones BK, Ahmad CS, Hung CT, Ateshian GA. Wear and damage of articular cartilage with friction against orthopedic implant materials. J Biomech. 2015; 48:1957–1964. DOI: 10.1016/j.jbiomech.2015.04.008 [PubMed: 25912663]

36. Pallante AL, Görtz S, Chen AC, Healey RM, Chase DC, Ball ST, Amiel D, Sah RL, Bugbee WD. Treatment of Articular Cartilage Defects in the Goat with Frozen Versus Fresh Osteochondral Allografts: Effects on Cartilage Stiffness, Zonal Composition, and Structure at Six Months. J Bone Jt Surg Am. 2012; 94:1984–1995. DOI: 10.2106/JBJS.K.00439

37. Wimmer MA, Grad S, Kaup T, Hänni M, Schneider E, Gogolewski S, Alini M. Tribology approach to the engineering and study of articular cartilage. Tissue Eng. 2004; 10:1436–1445. DOI: 10.1089/ten.2004.10.1436 [PubMed: 15588403]

38. Caligaris M, Ateshian GA. Effects of sustained interstitial fluid pressurization under migrating contact area, and boundary lubrication by synovial fluid, on cartilage friction. Osteoarthritis Cartilage. 2008; 16:1220–1227. DOI: 10.1016/j.joca.2008.02.020 [PubMed: 18395475]

39. Kaupp JA, Tse MY, Pang SC, Kenworthy G, Hetzler M, Waldman SD. The effect of moving point of contact stimulation on chondrocyte gene expression and localization in tissue engineered constructs. Ann Biomed Eng. 2013; 41:1106–1119. DOI: 10.1007/s10439-013-0763-0 [PubMed: 23417513]

40. Shekhawat, VK. Doctoral Dissertation. University of Illinois; Chicago: 2009. Influence of kinematics on mechano-biological response of articular cartilage - an in vitro investigation (PhD Dissertation). http://hdl.handle.net/10027/13472

41. Custers RJH, Saris DBF, Creemers LB, Verbout AJ, van Rijen MHP, Mastbergen SC, Lafeber FP, Dhert WJA. Replacement of the medial tibial plateau by a metallic implant in a goat model. J Orthop Res. 2010; 28:429–435. DOI: 10.1002/jor.21021 [PubMed: 19885911]

42. Clements KM, Bee ZC, Crossingham GV, Adams MA, Sharif M. How severe must repetitive loading be to kill chondrocytes in articular cartilage? Osteoarthritis Cartilage. 2001; 9:499–507. DOI: 10.1053/joca.2000.0417 [PubMed: 11467899]

43. Shekhawat VK, Laurent MP, Muehleman C, Wimmer MA. Surface topography of viable articular cartilage measured with scanning white light interferometry. Osteoarthritis Cartilage. 2009; 17:1197–1203. DOI: 10.1016/j.joca.2009.03.013 [PubMed: 19349041]

44. Abramoff PJMMD. Image processing with ImageJ. Biophotonics Int. 2003; 11:36–42.

45. Buckwalter JA. Articular Cartilage. Instr Course Lect. 1983; 32:349–370. [PubMed: 6085932]

46. Junqueira LC, Bignolas G, Brentani RR. Picrosirius staining plus polarization microscopy, a specific method for collagen detection in tissue sections. Histochem J. 1979; 11:447–455. [PubMed: 91593]

47. Masuda K, Shirota H, Thonar EJ. Quantification of 35S-labeled proteoglycans complexed to alcian blue by rapid filtration in multiwell plates. Anal Biochem. 1994; 217:167–175. DOI: 10.1006/abio.1994.1105 [PubMed: 7515600]

48. Farndale RW, Buttle DJ, Barrett AJ. Improved quantitation and discrimination of sulphated glycosaminoglycans by use of dimethylmethylene blue. Biochim Biophys Acta. 1986; 883:173–177. [PubMed: 3091074]

49. Chandrasekhar S, Esterman MA, Hoffman HA. Microdetermination of proteoglycans and glycosaminoglycans in the presence of guanidine hydrochloride. Anal Biochem. 1987; 161:103–108. DOI: 10.1016/0003-2697(87)90658-0 [PubMed: 3578776]

50. Brown S, Worsfold M, Sharp C. Microplate assay for the measurement of hydroxyproline in acid-hydrolyzed tissue samples. BioTechniques. 2001; 30:38–40. 42. [PubMed: 11196318]

51. Tortorella MD, Pratta M, Liu RQ, Austin J, Ross OH, Abbaszade I, Burn T, Arner E. Sites of aggrecan cleavage by recombinant human aggrecanase-1 (ADAMTS-4). J Biol Chem. 2000; 275:18566–18573. DOI: 10.1074/jbc.M909383199 [PubMed: 10751421]

52. Larsson S, Englund M, Struglics A, Lohmander LS. Association between synovial fluid levels of aggrecan ARGS fragments and radiographic progression in knee osteoarthritis. Arthritis Res Ther. 2010; 12:R230.doi: 10.1186/ar3217 [PubMed: 21194461]

53. Larsson S, Lohmander LS, Struglics A. An ARGS-aggrecan assay for analysis in blood and synovial fluid. Osteoarthritis Cartilage. 2014; 22:242–249. DOI: 10.1016/j.joca.2013.12.010 [PubMed: 24361794]

54. Grad S, Eglin D, Alini M, Stoddart MJ. Physical Stimulation of Chondrogenic Cells In Vitro: A Review. Clin Orthop Relat Res. 2011; 469:2764–2772. DOI: 10.1007/s11999-011-1819-9 [PubMed: 21344272]

55. Yusoff N, Abu Osman NA, Pingguan-Murphy B. Design and validation of a bi-axial loading bioreactor for mechanical stimulation of engineered cartilage. Med Eng Phys. 2011; 33:782–788. DOI: 10.1016/j.medengphy.2011.01.013 [PubMed: 21356602]

56. McCann L, Udofia I, Graindorge S, Ingham E, Jin Z, Fisher J. Tribological testing of articular cartilage of the medial compartment of the knee using a friction simulator. Tribol Int. 2008; 41:1126–1133. DOI: 10.1016/j.triboint.2008.03.012

57. Hodge WA, Fijan RS, Carlson KL, Burgess RG, Harris WH, Mann RW. Contact pressures in the human hip joint measured in vivo. Proc Natl Acad Sci U S A. 1986; 83:2879–2883. [PubMed: 3458248]

58. Tackson SJ, Krebs DE, Harris BA. Acetabular pressures during hip arthritis exercises. Arthritis Care Res Off J Arthritis Health Prof Assoc. 1997; 10:308–319.

59. Gilbert S, Chen T, Hutchinson ID, Choi D, Voigt C, Warren RF, Maher SA. Dynamic contact mechanics on the tibial plateau of the human knee during activities of daily living. J Biomech. 2014; 47:2006–2012. DOI: 10.1016/j.jbiomech.2013.11.003 [PubMed: 24296275]

60. Torzilli PA, Grigiene R. Continuous cyclic load reduces proteoglycan release from articular cartilage. Osteoarthritis Cartilage. 1998; 6:260–268. DOI: 10.1053/joca.1998.0119 [PubMed: 9876395]

61. Torzilli PA, Bhargava M, Park S, Chen CTC. Mechanical load inhibits IL-1 induced matrix degradation in articular cartilage. Osteoarthritis Cartilage. 2010; 18:97.doi: 10.1016/j.joca. 2009.07.012 [PubMed: 19747586]

62. Hayes A, Harris B, Dieppe PA, Clift SE. Wear of articular cartilage: the effect of crystals. Proc Inst Mech Eng [H]. 1993; 207:41–58.

63. Newberry WN, Garcia JJ, Mackenzie CD, Decamp CE, Haut RC. Analysis of acute mechanical insult in an animal model of post-traumatic osteoarthrosis. J Biomech Eng. 1998; 120:704–709. [PubMed: 10412452]

64. Minihane KP, Turner TM, Urban RM, Williams JM, Thonar EJ-M, Sumner DR. Effect of hip hemiarthroplasty on articular cartilage and bone in a canine model. Clin Orthop. 2005:157–163.

65. Forster H, Fisher J. The influence of continuous sliding and subsequent surface wear on the friction of articular cartilage. Proc Inst Mech Eng [H]. 1999; 213:329–345.

66. McGann ME, Vahdati A, Wagner DR. Methods to assess in vitro wear of articular cartilage. Proc Inst Mech Eng [H]. 2012; 226:612–622.

67. Chan SMT, Neu CP, DuRaine G, Komvopoulos K, Reddi AH. Tribological altruism: A sacrificial layer mechanism of synovial joint lubrication in articular cartilage. J Biomech. 2012; 45:2426–2431. DOI: 10.1016/j.jbiomech.2012.06.036 [PubMed: 22867761]

68. Bonassar LJ, Grodzinsky AJ, Frank EH, Davila SG, Bhaktav NR, Trippel SB. The effect of dynamic compression on the response of articular cartilage to insulin-like growth factor-I. J Orthop Res. 2001; 19:11–17. DOI: 10.1016/S0736-0266(00)00004-8 [PubMed: 11332605]

69. Evans RC, Quinn TM. Dynamic compression augments interstitial transport of a glucose-like solute in articular cartilage. Biophys J. 2006; 91:1541–1547. DOI: 10.1529/biophysj.105.080366 [PubMed: 16679370]

70. Malfait AM, Ritchie J, Gil AS, Austin J-S, Hartke J, Qin W, Tortorella MD, Mogil JS. ADAMTS-5 deficient mice do not develop mechanical allodynia associated with osteoarthritis following medial meniscal destabilization. Osteoarthritis Cartilage. 2010; 18:572–580. DOI: 10.1016/j.joca. 2009.11.013 [PubMed: 20036347]

71. Dufield DR, Nemirovskiy OV, Jennings MG, Tortorella MD, Malfait AM, Mathews WR. An immunoaffinity liquid chromatography-tandem mass spectrometry assay for detection of endogenous aggrecan fragments in biological fluids: Use as a biomarker for aggrecanase activity and cartilage degradation. Anal Biochem. 2010; 406:113–123. DOI: 10.1016/j.ab.2010.06.044 [PubMed: 20603097]

72. Bay-Jensen AC, Reker D, Kjelgaard-Petersen CF, Mobasheri A, Karsdal MA, Ladel C, Henrotin Y, Thudium CS. Osteoarthritis year in review 2015: soluble biomarkers and the BIPED criteria. Osteoarthritis Cartilage. 2016; 24:9–20. DOI: 10.1016/j.joca.2015.10.014 [PubMed: 26707988]

73. Steinmeyer J, Knue S. The proteoglycan metabolism of mature bovine articular cartilage explants superimposed to continuously applied cyclic mechanical loading. Biochem Biophys Res Commun. 1997; 240:216–221. DOI: 10.1006/bbrc.1997.7641 [PubMed: 9367913]

74. Sauerland K, Raiss RX, Steinmeyer J. Proteoglycan metabolism and viability of articular cartilage explants as modulated by the frequency of intermittent loading. Osteoarthritis Cartilage. 2003; 11:343–350. [PubMed: 12744940]

75. Olivier P, Loeuille D, Watrin A, Walter F, Etienne S, Netter P, Gillet P, Blum A. Structural evaluation of articular cartilage: potential contribution of magnetic resonance techniques used in clinical practice. Arthritis Rheum. 2001; 44:2285–2295. [PubMed: 11665969]

76. Levin AS, Chen C-TC, Torzilli PA. Effect of tissue maturity on cell viability in load-injured articular cartilage explants. Osteoarthr Cartil OARS Osteoarthr Res Soc. 2005; 13:488–496. DOI: 10.1016/j.joca.2005.01.006

77. Torzilli PA, Deng X-H, Ramcharan M. Effect of compressive strain on cell viability in statically loaded articular cartilage. Biomech Model Mechanobiol. 2006; 5:123–132. DOI: 10.1007/s10237-006-0030-5 [PubMed: 16506016]

78. Mündermann A, Dyrby CO, Andriacchi TP, King KB. Serum concentration of cartilage oligomeric matrix protein (COMP) is sensitive to physiological cyclic loading in healthy adults. Osteoarthritis Cartilage. 2005; 13:34–38. DOI: 10.1016/j.joca.2004.09.007 [PubMed: 15639635]

79. Erhart-Hledik JC, Favre J, Asay JL, Smith RL, Giori NJ, Mündermann A, Andriacchi TP. A relationship between mechanically-induced changes in serum cartilage oligomeric matrix protein (COMP) and changes in cartilage thickness after 5 years. Osteoarthritis Cartilage. 2012; 20:1309–1315. DOI: 10.1016/j.joca.2012.07.018 [PubMed: 22868052]

80. Kumahashi N, Swärd P, Larsson S, Lohmander LS, Frobell R, Struglics A. Type II collagen C2C epitope in human synovial fluid and serum after knee injury--associations with molecular and structural markers of injury. Osteoarthritis Cartilage. 2015; 23:1506–1512. DOI: 10.1016/j.joca.2015.04.022 [PubMed: 25937025]
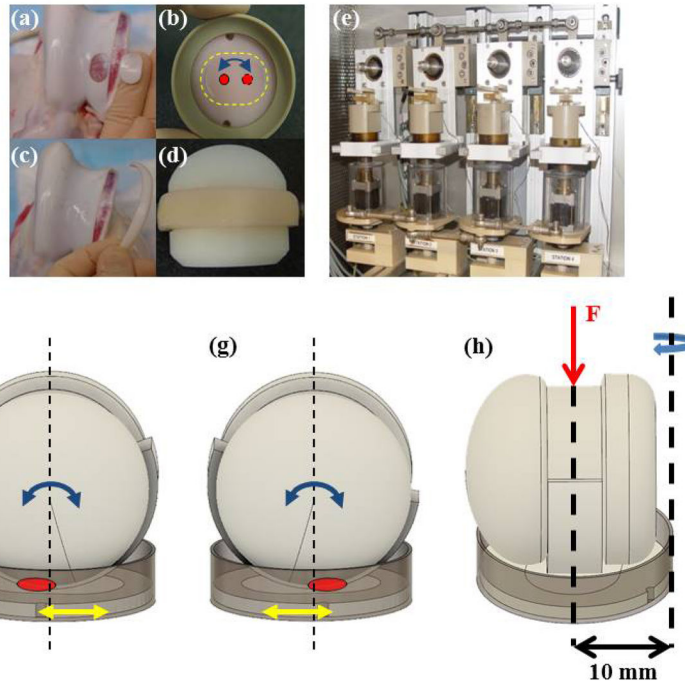
Figure 1.
Image of the disc removed from trochlear groove (a) and secured in semi-confined compression in the polyethylene wafer in a PEEK cup (b). Image of the cartilage strip removed from the trochlear rim (c) and then secured to the polyethylene ball adapted (d). (e) Image of the tribological testing device housed in an incubator where the ball set at the top of the station and rotated at a frequency of 0.5 Hz and a stroke of 30° while the explant rotated at 0.1 Hz and a stroke of 15°. This motion with a contact area of roughly 20 mm^2 creates a 5.2 mm curvilinear wear path. (f–g) Diagram of the migrating contact point (red circle) on the cartilage disc surface through dual-axial rotation of the disc/cup (yellow arrow) and of the strip/ball (blue arrow), which can also be seen from contact points marked in Figure 1b. (h) The curvilinear translation shown in Figures 1b, 1f, and 1g was technically realized through offsetting the rotational axis of the disc from the loading axis by 10 mm.
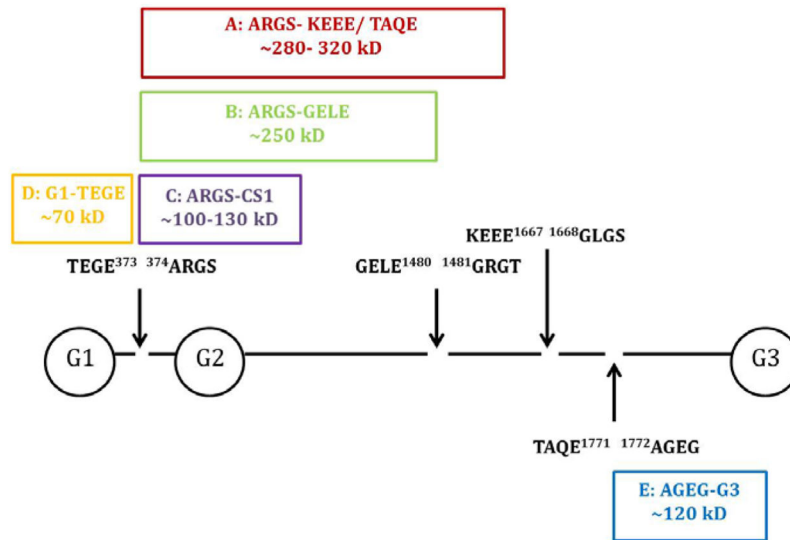
Figure 2.
Schema of the aggrecan core protein (with GAG chains removed)[51–52]. AHP0022 detects bands A–D and anti-AGEG detects band E. Arrows delineate definite ADAMTS cleavage sites for bands A, B, D, and E[51] while bands A–E are all detectable aggrecan fragments. G1, G2, G3 represent the globular domains.
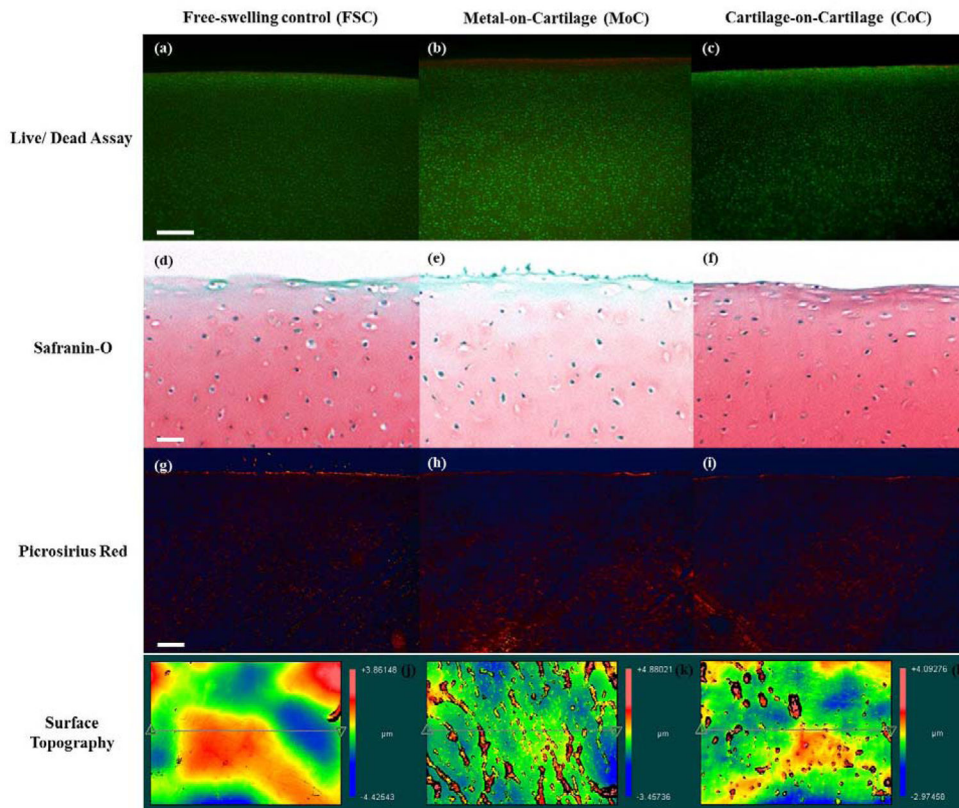
Figure 3.
Live/dead cross-sections of the cartilage explants from (a) FSC, (b) MoC, and (c) CoC groups stained with calcein AM (green; living chondrocytes) and ethidium homodimer (red; dead chondrocytes) at 5x. Representative cross-sections of the cartilage explants from (d) FSC, (e) MoC, and (f) CoC groups stained with Safranin-O for GAG at 4x magnification. Representative cross-sections of the cartilage explants from (g) FSC, (h) MoC, and (i) CoC groups stained with Picrosirius red for collagen at 4x magnification. Representative topographical plots of average SRz values for (j) FSC, (k) MoC, and (l) CoC. (g) represents the native microfeatures of cartilage, while (h) displays an increase in microfibrillation features as compared to (g)and (i). Bar represents 250 μm.
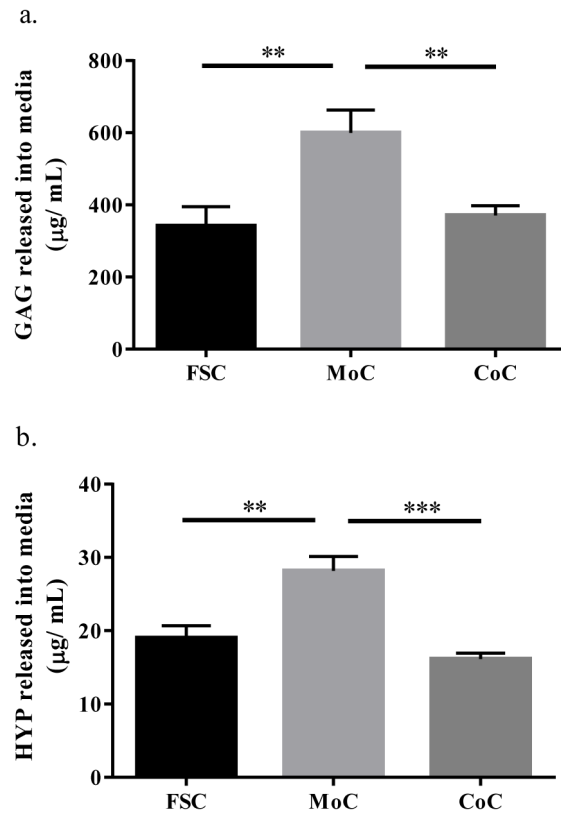
a.

b.

Figure 4.
(a) GAG released into the media. (b) HYP released into the media. CoC samples are corrected to account for two interacting cartilage surfaces which both release matrix contents into the media. Data represents means +/− SEM for n=10–12 explants. **: p<0.01, ***: p<0.001 as compared to MoC.

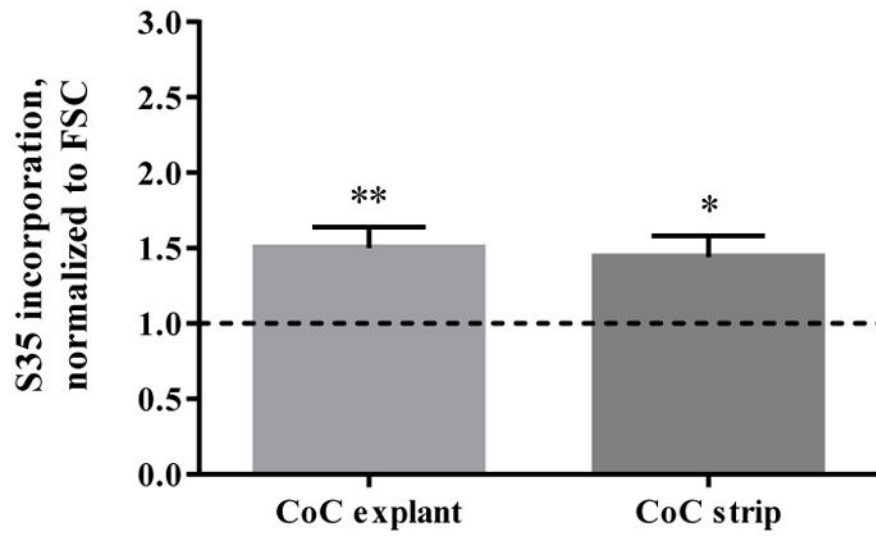**Figure 5.**
Radiolabeled $^{35}SO_4$-incorporation for live CoC articulated explants and strips, normalized to live FSC. Dotted line represents FSC. Data represents means +/− SEM for n=8 explants and strips. *: $p<0.05$, **: $p<0.01$ as compared to FSC.

a.

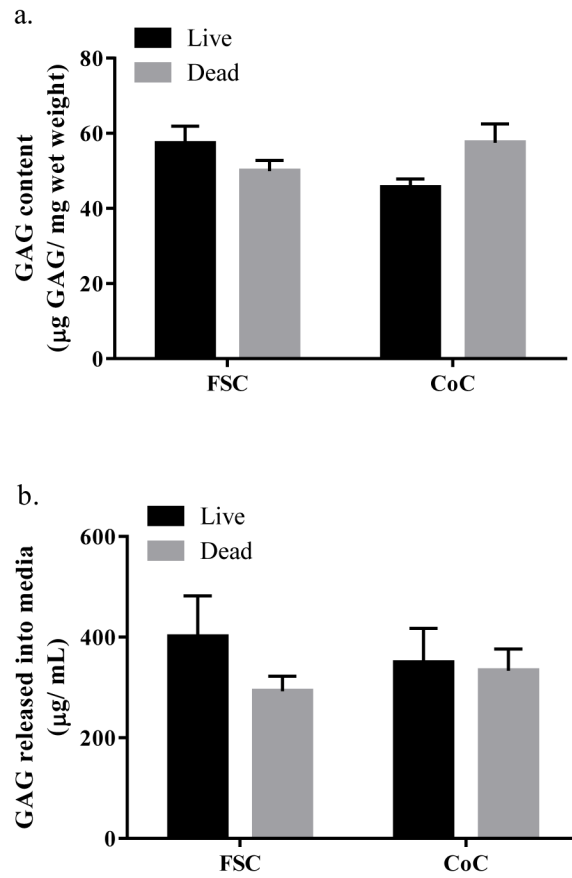

b.

Figure 6.
(a) GAG content of cartilage plugs. (b) GAG released into media. Data represents means +/−
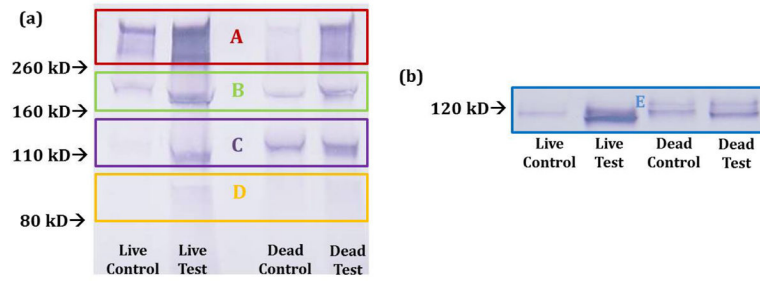SEM for n=6 (GAG content) and n=12 (GAG release).

Figure 7.
Western blot results from the use of the antibody AHP0022 (a) and anti-AGEG (b). AHP0022 resulted in multiple bands as the antibody is to the interglobular domains in G1 and G2. Anti-AGEG resulted in a single band representing a specific aggrecan fragment. At least two samples were run per condition to confirm Western blot results. Figure 2 serves as the band reference.

Table 1

Cell viability in the superficial zone (SZ: top 15% of the tissue) and total depth of tissue.

	Superficial Zone Viability (%)	Total Depth Viability (%)
FSC	85.87 +/− 1.95	86.68 +/− 2.13
MoC	**44.83 +/− 5.56** [****]	**60.60 +/− 3.16** [****]

Data represents means +/− SEM for n=10–12 explants.

[****] p<0.0001 as compared to FSC.

Author Manuscript

Author Manuscript

Author Manuscript

Author Manuscript

Table 2

Summary of surface roughness values for FSC and articulated samples.

	Ra (nm)	SRz (μm)	Rsk (nm)	PV (μm)
FSC	0.477 +/−0.045	1.41 +/− 0.147	0.327 +/− 0.117	7.50 +/− 1.09
MoC	0.522 +/− 0.066	**2.76 +/− 0.284**[**]	0.505 +/− 0.163	10.75 +/− 0.706
CoC	0.428 +/− 0.047	2.19 +/− 0.283	0.536 +/− 0.359	10.76 +/− 1.35

Ra: Arithmetical mean deviation roughness, SRz: Average radial peak-to-valley areal roughness, Rsk: areal skewness of the roughness (positive skew indicates a predominance of peaks), and PV: peak to valley difference. Data represents means +/− SEM for n=10–12 explants.

[**] p<0.01 as compared to FSC.

Table 3

Cell viability in the superficial zone (SZ: top 15% of the tissue) and total depth of tissue.

	Superficial Zone Viability (%)	Total Depth Viability (%)
FSC	74.36 +/− 2.53	71.62 +/− 2.53
CoC explant	71.21 +/− 3.74	73.29 +/− 2.73
CoC strip	61.09 +/− 5.02	60.97 +/− 3.63

Data represents means +/− SEM for n=7–8 explants.